

Beamforming Design and Power Allocation for Secure Transmission with NOMA

Youhong Feng, *Student Member, IEEE*, Shihao Yan, *Member, IEEE*, Zhen Yang,
Nan Yang, *Member, IEEE*, and Jinhong Yuan, *Fellow, IEEE*

Abstract

In this work, we propose a novel beamforming design to enhance physical layer security of a non-orthogonal multiple access (NOMA) system with the aid of artificial noise (AN). The proposed design uses two scalars to balance the useful signal strength and interference at the strong and weak users, which is a generalized version of the existing beamforming designs in the context of physical layer security for NOMA. We determine the optimal power allocation among useful signals and AN together with the two optimal beamforming scalars in order to maximize the secrecy sum rate (SSR). Our asymptotic analysis in the high signal-to-noise ratio regime provides an efficient and near-optimal solution to optimizing the beamforming scalars and power allocation coefficients. Our analysis indicates that it is not optimal to form a beam towards either the strong user or the weak user in NOMA systems for security enhancement. In addition, the asymptotically optimal power allocation informs that, as the transmit power increases, more power should be allocated to the weak user or AN signals, while the power allocated to the strong user keeps constant. Our examination shows that the proposed novel beamforming design can significantly outperform two benchmark schemes.

Index Terms

Non-orthogonal multiple access, physical layer security, artificial noise, optimal power allocation.

This work was partially supported by the National Natural Science Foundation of China (No.61772287, 61671252).

Y. Feng and Z. Yang are with the Key Laboratory of Ministry of Education in Broadband Wireless Communication and Sensor Network Technology, Nanjing University of Posts and Telecommunications, Nanjing 210003, China (e-mails: {2013010213, yangz}@njupt.edu.cn). Y. Feng is also with the College of Physics and Electronic information Engineering, Anhui Normal University, Wuhu 241000, China, and the Research School of Engineering, Australian National University, Canberra, ACT, Australia. S. Yan is with the School of Engineering, Macquarie University, NSW 2109, Australia (e-mail:shihao.yan@mq.edu.au). N. Yang is with the Research School of Engineering, Australian National University, Canberra, ACT 2600, Australia (email: nan.yang@anu.edu.au). J. Yuan is with the School of Electrical Engineering and Telecommunications, The University of New South Wales, Sydney, NSW 2052, Australia (e-mail: j.yuan@unsw.edu.au).

I. INTRODUCTION

Non-orthogonal multiple access (NOMA), as a potentially promising technique to significantly boost the system spectral efficiency in the fifth-generation (5G) and beyond wireless networks, has attracted an increasing amount of research effort [1]–[4]. Different from the conventional orthogonal multiple access (OMA) techniques, such as frequency division multiple access, time division orthogonal multiple access, and code division multiple access, NOMA can exploit the power domain to serve multiple users simultaneously in the same resource block (i.e., time/frequency/code), in which successive interference cancellation (SIC) is widely applied. Motivated by the improved spectral efficiency provided by NOMA, different issues in NOMA systems have been addressed in the literature (e.g., [5]–[9]). For example, [5] focused on a down-link NOMA system, where the authors considered user pairing and transmit power allocation to enhance the performance of NOMA. In [6], an optimal transmit power allocation scheme was proposed in multiple-input multiple-output (MIMO) NOMA systems in order to maximize the sum rate of two paired users subject to some specific constraints. In addition, the authors of [7] proposed a joint subcarrier and power allocation scheme to maximize the weighted sum rate of a NOMA system. Considering delay constraint, the authors of [8] tackled the maximization of the effective throughput in the context of NOMA for short-packet communications, which shows that NOMA can aid to achieve low-latency communications.

Wireless communication security is another critical issue of growing importance in 5G and beyond wireless networks, since there is an increasing amount of confidential information (e.g., credit card information) that is transferred over the air. Physical layer security, as a complementary and alternative cryptographic method to defend against eavesdroppers, exploits the inherent properties (e.g., randomness) of the wireless medium to achieve the ever-lasting and information-theoretic secrecy (e.g., [10]–[17]). In this context, MIMO architectures (e.g., [12], [13]) and artificial-noise (AN)-aided secure transmissions (e.g., [13]–[17]) have been widely adopted to enhance the secrecy performance of wireless communications. Against this background, physical layer security in NOMA systems has been partially addressed [18]–[27]. For example, in [20] the authors considered physical layer security in a single-input single-output (SISO) NOMA system

and proposed an optimal power allocation policy for maximizing the secrecy sum rate (SSR) of all users subject to their predefined quality of service (QoS) requirements. In [21], the authors focused on the transmission power minimization in a multiple-input single-output (MISO) NOMA cognitive radio network in the presence of multiple single-antenna eavesdroppers. Considering a cell-edge user (i.e., the weak user) as a potential eavesdropper to an entrusted central user (i.e., the strong user), the maximization of the secrecy rate of the central user subject to a transmit power constraint and a transmission rate requirement at the cell-edge user is tackled in [22]. In [23], the authors focused on the SSR optimization problem for a downlink MIMO NOMA network subject to successful SIC and transmit power constraints, in which the nonconvex maximization of the SSR was transfer to a biconvex problem that was solved by alternating optimization method.

In the considered NOMA systems of [21]–[23], either the perfect knowledge on the eavesdropper’s instantaneous channel state information (CSI) or a bounded error model on the the eavesdropper’s instantaneous CSI was considered. Such CSI information may not be achievable in some specific application scenarios of NOMA, in which the eavesdropper is not an internal user or an active receiver. As such, the assumption that only the statistical information on the eavesdropper’s CSI (e.g., a passive eavesdropping scenario) was widely used in the context of physical layer security for NOMA (e.g., [24]–[26]). Specifically, [24] proposed a NOMA scheme that maximizes the minimum confidential information rate under the secrecy outage probability (SOP) and transmit power constraints. Inspired by the enhanced secrecy performance achieved by AN-aided transmission strategies, [25] and [26] considered AN-aided secure beamforming (SBF) strategies to protect the confidential information of legitimate users for MISO NOMA systems. More specifically, the authors of [25] considered large-scale networks with randomly deployed legitimate users and eavesdroppers, where the exact and asymptotic expressions for the SOP were derived. The imperfect SIC was considered in [26], where the SOPs of the legitimate users were obtained in closed-form expressions.

With regard to the SBF design in NOMA systems, in [25] a maximum ratio transmission (MRT) strategy was adopted, i.e., $\mathbf{v}_1 = \mathbf{h}_1/|\mathbf{h}_1|$ and $\mathbf{v}_2 = \mathbf{h}_2/|\mathbf{h}_2|$, where \mathbf{v}_1 and \mathbf{v}_2 are the

beamforming vectors used to transmit useful signals to the weak user (User 1) and the strong user (User 2), respectively, while \mathbf{h}_1 and \mathbf{h}_2 are the channel vectors from the transmitter to User 1 and User 2, respectively. In this MRT strategy, the signal strengths of s_1 and s_2 are maximized at User 1 and User 2, respectively. As clarified in [26], this MRT strategy may not guarantee perfect SIC at User 2 (i.e., the strong user), since the interference caused by s_2 is also maximized when User 2 decodes s_1 in order to conduct SIC. Thus, in [26] the SBF is designed such that $\mathbf{v}_1 = \mathbf{v}_2 = \mathbf{h}_2/|\mathbf{h}_2|$, i.e., the signal strengths of both s_1 and s_2 are maximized at User 2. In the SBF designs proposed by [25] and [26], we observe that the freedom of balancing the useful signal strength and interference is lost, i.e., the useful signal strengths and interference are either minimized or maximized. We note that this freedom can potentially enhance the achieved physical layer security in NOMA systems, since the useful signal s_1 should be decoded at both User 1 and User 2, while the useful signal s_2 causes interference at both User 1 and User 2 (but s_2 is only decoded at User 2). To design a SBF, for which the freedom to balance useful signal strengths and interference can be achieved in order to improve the secrecy performance of NOMA systems, motivates this work and our main contributions are summarized as below.

- We propose a novel hybrid SBF scheme in a NOMA system, which can balance the useful signal strengths and interference at both User 1 and User 2 in order to enhance physical layer security. Specifically, in our proposed scheme \mathbf{v}_1 is a linear function of \mathbf{h}_1 and \mathbf{h}_2 , which is determined by a parameter β_1 , and \mathbf{v}_2 is a linear function of \mathbf{h}_1 and \mathbf{e} , which is determined by another parameter β_2 , where \mathbf{e} is random vector that does not align with \mathbf{h}_1 or \mathbf{h}_2 . In this scheme, AN is also used to further enhance the secrecy performance of NOMA systems and thus we refer to this scheme as the NOMA-HB-AN scheme, in which the beams used to transmit s_1 and s_2 can be flexibly controlled to be in any direction (e.g., maybe towards neither User 1 nor User 2). We note that the proposed NOMA-HB-AN scheme is a generalized version of the SBF designs proposed in [25] and [26].
- In order to maximize the benefits of the proposed NOMA-HB-AN scheme, we tackle the optimization of the two governing parameters β_1 and β_2 together with the optimal power allocation among s_1 , s_2 , and the AN signals, aiming to maximize the SSR subject to

specific QoS constraints at the two legitimate users. Considering a larger number of transmit antennas, we first determine the optimal power allocation for given β_1 and β_2 , in which the power allocation coefficients for s_1 and s_2 are analytically derived as functions of the power allocation coefficient for AN signals. This leads to that the optimal power allocation can be achieved with the aid of a one-dimensional numerical search. Our examination shows that the proposed NOMA-HB-AN scheme can significantly outperform the SBF design with $\mathbf{v}_1 = \mathbf{v}_2 = \mathbf{h}_2/|\mathbf{h}_2|$ proposed in [26].

- To gain further insights on the proposed scheme, we consider the joint optimization of β_1 and β_2 together with power allocation in the regime of high signal-to-noise (SNR) ratio. Particularly, we derive the power allocation coefficients for s_1 , s_2 , and the AN signals in closed-form expressions in the high-SNR regime, based on which the optimization of β_1 and β_2 can be efficiently achieved by another one-dimensional numerical search. Our numerical examination shows that the achieved optimal β_1 , β_2 , and power allocation in the high-SNR regime can precisely approximate those achieved for arbitrary SNRs, in terms of achieving similar maximum SSRs. This indicates that our proposed SBF design can be efficiently optimized and the associated complexity increase is negligible. Our results also show that, when the eavesdropper's channel quality is not that high, the design of SBF is more important than whether to use AN, which is confirmed by our observation that the proposed SBF design without AN can even outperform the design with $\mathbf{v}_1 = \mathbf{v}_2 = \mathbf{h}_2/|\mathbf{h}_2|$ and AN.

The remainder of this paper is organized as follows. In Section II, the system model and the hybrid SBF are presented. The maximization of the SSR under the QoS constraints at the two legitimate users is formulated in Section III. The solution to the SSR maximization problem are provided in Section IV, where the scenarios with arbitrary and high SNRs are considered. Numerical results are provided in Section V to offer valuable insights on the secrecy performance of the proposed scheme compared with two benchmark schemes. Conclusions are drawn in Section VI.

Notation: Scalar variables are denoted by italic symbols; Vectors and matrices are denoted by

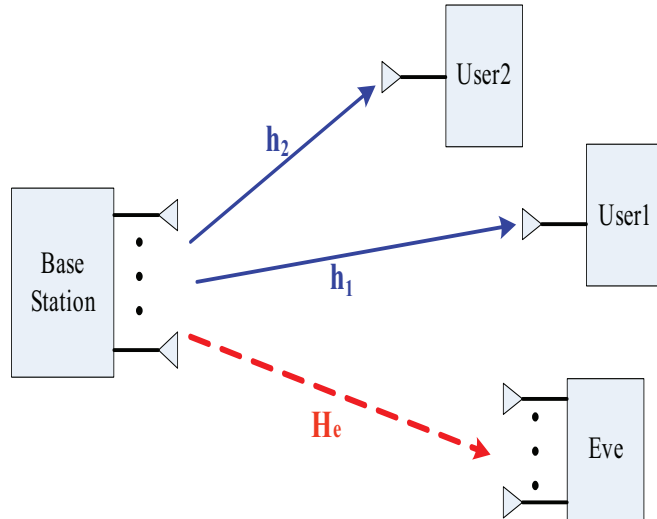


Fig. 1. Illustration of a downlink MISOME NOMA system, where the BS is equipped with N antennas, each of User 1 and User 2 is equipped with a single antenna, and the eavesdropper is equipped with K antenna.

lower-case and upper-case boldface symbols, respectively; \mathbf{A}^H denotes the Hermitian (conjugate) transpose of a matrix \mathbf{A} ; \mathbf{I}_K represents the $K \times K$ identity matrix; $E[x]$ denote the mean of the random variable x ; $x \sim CN(\mu, \sigma^2)$ denotes a circularly symmetric complex Gaussian random variable x with mean μ and covariance σ^2 .

II. SYSTEM MODEL

We consider the secure transmission using NOMA from a base station (BS) to two legitimate users in the presence of a multi-antenna eavesdropper (Eve). The BS is equipped with N antennas, each of the legitimate users (i.e., User 1 and User 2) is equipped with a single antenna, and Eve is equipped with K antennas. As such, we refer to the considered system as a MISOME NOMA system. We assume that N is large, and in particular is much larger than K . The channel vector from the BS to the legitimate user $m \in \{1, 2\}$ is denoted by $\mathbf{h}_m \in \mathbb{C}^{1 \times N}$, of which the entries are independent and identically distributed (i.i.d.) circularly-symmetric complex Gaussian random variables with zero-mean and variance δ_m^2 . The channel matrix from the BS to Eve is denoted by $\mathbf{H}_e \in \mathbb{C}^{K \times N}$, where $\mathbf{h}_{e,k} \triangleq \mathbf{H}_e(k, :)$ and $\mathbf{h}_{e,k} \in \mathbb{C}^{1 \times N}$ is an $1 \times N$ channel vector from the BS to the k -th receive antenna at Eve and $\mathbf{h}_{e,k}$ is i.i.d. circularly-symmetric complex Gaussian entries with zero-mean and variance δ_e^2 .

In this work, we assume that the CSI of all the legitimate channels (i.e., \mathbf{h}_m) is known at the BS, while only the statistical CSI of the Eve's channel (i.e., the statistical information on \mathbf{H}_e) is available. It is a very generic assumption that the statistical CSI of the Eve's channel is known, which has been widely adopted in the literature of physical layer security [26], [29], [30]. Without loss of generality, we assume that the legitimate channel gains are sorted in ascending order [24], [27], i.e., $0 < \|\mathbf{h}_1\|^2 \leq \|\mathbf{h}_2\|^2$.

A. Secure Transmission with NOMA and Artificial Noise

We next detail the secure transmission using NOMA with AN in our considered system model. Specifically, the BS transmits two information signals, s_1 and s_2 , in conjunction with an $(N - 2) \times 1$ AN vector \mathbf{s}_N to its corresponding receivers, where s_m is the information signal dedicated for the m -th user. The variance of s_m is denoted by χ_m and the total transmit power is denoted by P . We denote ϕ_m as the power allocation coefficient to s_m , where $0 < \phi_m \leq 1$, which determines the fraction of the total transmit power allocated to s_m such that $\chi_m = \phi_m P$. Since the BS does not know \mathbf{H}_e , it equally distributes the AN transmit power to each entry of \mathbf{s}_N and thus the variance of each entry of \mathbf{s}_N is the same, which is denoted by χ_N . Then the BS transmits \mathbf{s}_N in the null space of the channel from the BS to the two users, $\mathbf{H} \triangleq [\mathbf{h}_1^H, \mathbf{h}_2^H]$, such that \mathbf{s}_N leads to interference at Eve but not at the two legitimate users. As such, we know that all the remaining transmit power (excluding the power allocated to s_1 and s_2) should be used to transmit \mathbf{s}_N , such that we have $\chi_N = \phi_e P / (N - 2)$ with $\phi_e = 1 - \phi_1 - \phi_2$. To transmit s_m and \mathbf{s}_N , the BS has to design an $N \times N$ beamforming matrix \mathbf{V} given by

$$\mathbf{V} = [\mathbf{v}_1, \mathbf{v}_2, \mathbf{V}_N], \quad (1)$$

where we recall that \mathbf{v}_1 and \mathbf{v}_2 are the beamforming vectors used to transmit s_1 and s_2 , respectively, and \mathbf{V}_N is the unitary beamforming matrix used to transmit \mathbf{s}_N . In this work, we adopt specific structures for \mathbf{v}_1 and \mathbf{v}_2 given as

$$\mathbf{v}_1 = \frac{\sqrt{\beta_1} \hat{\mathbf{h}}_1 + \sqrt{(1 - \beta_1)} \hat{\mathbf{h}}_2}{\|\sqrt{\beta_1} \hat{\mathbf{h}}_1 + \sqrt{(1 - \beta_1)} \hat{\mathbf{h}}_2\|}, \quad (2)$$

$$\mathbf{v}_2 = \frac{\sqrt{\beta_2} \hat{\mathbf{h}}_2 + \sqrt{(1 - \beta_2)} \hat{\mathbf{e}}}{\|\sqrt{\beta_2} \hat{\mathbf{h}}_2 + \sqrt{(1 - \beta_2)} \hat{\mathbf{e}}\|}, \quad (3)$$

where β_1 and β_2 are design parameters to be determined later, $\hat{\mathbf{h}}_i = \frac{\mathbf{h}_i}{\|\mathbf{h}_i\|}$, $\hat{\mathbf{e}} = \frac{\mathbf{e}}{\|\mathbf{e}\|}$, and $\mathbf{e} \in \mathbb{C}^{1 \times N}$ is a random vector that does not align with \mathbf{h}_1 or \mathbf{h}_2 . The design of \mathbf{v}_1 originates from the fact that the information signal s_1 need to be decoded by both User 1 and User 2 (User 2 decodes s_1 by performing SIC) and the design of \mathbf{v}_2 originates from that only User 2 decodes s_2 while s_2 causes interference at User 1 for decoding s_1 . We note that the proposed \mathbf{v}_1 and \mathbf{v}_2 are generalizations of the beamforming vectors adopted in existing works (e.g., [25], [26]) and thus they are expected to achieve better system performance with optimized β_1 and β_2 , which will be confirmed by our examination in this work. Using \mathbf{V} , the transmitted signal vector at the BS is given by

$$\mathbf{s} = \mathbf{V} \begin{bmatrix} s_1 \\ s_2 \\ \mathbf{s}_N \end{bmatrix} = \mathbf{v}_1 s_1 + \mathbf{v}_2 s_2 + \mathbf{V}_N \mathbf{s}_N. \quad (4)$$

Therefore, the received signal at the m -th user is given by

$$\begin{aligned} y_m &= \mathbf{h}_m \mathbf{s} + n_m \\ &= \mathbf{h}_m \sum_{i=1}^2 \mathbf{v}_i s_i + \mathbf{h}_m \mathbf{V}_N \mathbf{s}_N + n_m \\ &= \mathbf{h}_m \sum_{i=1}^2 \mathbf{v}_i s_i + n_m, \end{aligned} \quad (5)$$

where n_m satisfying $E[n_m n_m^H] = \sigma_m^2$ is the additive white Gaussian noise (AWGN) at the m -th user and $\mathbf{h}_m \mathbf{V}_N = \mathbf{0}$ is applied, since \mathbf{s}_N is transmitted in the null space of \mathbf{H} . Likewise, the received signal vector at Eve is given by

$$\mathbf{y}_e = \mathbf{H}_e \mathbf{s} + \mathbf{n}_e = \mathbf{H}_e \sum_{i=1}^2 \mathbf{v}_i s_i + \mathbf{H}_e \mathbf{V}_N \mathbf{s}_N + \mathbf{n}_e, \quad (6)$$

where \mathbf{n}_e satisfying $E[\mathbf{n}_e \mathbf{n}_e^H] = \sigma_e^2 \mathbf{I}_K$ is the AWGN vector at Eve.

B. Performance Metric for NOMA with AN

According to the principle of NOMA, the user with the better channel condition (i.e., User 2) firstly decodes the signal of the other user (i.e., User 1) and then successively subtracts the interference caused by this signal from its received signal before decoding its own information.

The weak user, User 1 directly decodes its own information by treating User 2's signal as interference [31]. As such, the maximum achievable rate of s_1 is given by [26], [28]

$$R_{u1} = \log_2(1 + \gamma_{u1}), \quad (7)$$

where

$$\gamma_{u1} = \min \left(\frac{\phi_1 P |\mathbf{h}_1 \mathbf{v}_1|^2}{\phi_2 P |\mathbf{h}_1 \mathbf{v}_2|^2 + \sigma_1^2}, \frac{\phi_1 P |\mathbf{h}_2 \mathbf{v}_1|^2}{\phi_2 P |\mathbf{h}_2 \mathbf{v}_2|^2 + \sigma_2^2} \right), \quad (8)$$

while the first and second terms on the right-hand side of (8) denote the received SINR for decoding User 1's signal s_1 at User 1 and User 2, respectively. We note that the "min" function used in (8) comes from the assumption that perfect SIC is guaranteed at User 2, which is assumed in this work. With SIC, User 2 decodes its information signal without interference and thus, the maximum achievable rate of s_2 is given by

$$R_{u2} = \log_2(1 + \gamma_{u2}), \quad (9)$$

where $\gamma_{u2} = \phi_2 P |\mathbf{h}_2 \mathbf{v}_2|^2 / \sigma_2^2$ denotes the SNR for decoding User 2's signal at User 2.

In this work, we consider a worst-case scenario, where Eve has already decoded the information signal for User 1 in order to conduct SIC before it attempts to decode the information for User 2, which is exactly the same as the decoding procedure at User 2 (i.e., the strong user). The worst-case assumption has been widely adopted in designing and analyzing the NOMA transmission schemes with physical layer security (e.g., [20], [24]). As such, the maximum achievable rate of s_1 at Eve is given by [32], [34]

$$R_{e1} = \log_2 \det \left(\sigma_e^2 \mathbf{I}_K + \frac{\phi_1 P \mathbf{H}_e \mathbf{v}_1 (\mathbf{H}_e \mathbf{v}_1)^H}{\phi_2 P \mathbf{H}_e \mathbf{v}_2 (\mathbf{H}_e \mathbf{v}_2)^H + \frac{\phi_e P}{N-2} \mathbf{H}_e \mathbf{V}_N (\mathbf{H}_e \mathbf{V}_N)^H + \sigma_e^2 \mathbf{I}_K} \right). \quad (10)$$

Likewise, the maximum achievable rate of s_2 at Eve is given by [32], [34]

$$R_{e2} = \log_2 \det \left(\sigma_e^2 \mathbf{I}_K + \frac{\phi_2 P \mathbf{H}_e \mathbf{v}_2 (\mathbf{H}_e \mathbf{v}_2)^H}{\frac{\phi_e P}{N-2} \mathbf{H}_e \mathbf{V}_N (\mathbf{H}_e \mathbf{V}_N)^H + \sigma_e^2 \mathbf{I}_K} \right). \quad (11)$$

We denote the achievable secrecy rate of s_m and the SSR as R_{sm} and R_s , respectively. Therefore, we have

$$R_s = \sum_{m=1}^2 R_{sm} = \sum_{m=1}^2 [R_{um} - R_{em}]^+, \quad (12)$$

where $[x]^+ \triangleq \max(0, x)$. We note that the SSR normally cannot be adopted as the secrecy performance metric in the passive eavesdropping scenario, where the instantaneous CSI of the Eve's channel is unknown. However, as the number of transmit antennas (i.e., N) approaches infinity (which is the focus of this work), the CSI of the Eve's channel is asymptotically achievable. As such, following [33], [35] in this work we adopt the SSR as our performance metric under some specific constraints.

III. OPTIMIZATION FRAMEWORK WITH A SUFFICIENT LARGE NUMBER OF TRANSMIT ANTENNAS

In this section, we first present the adopted optimization framework. By considering a sufficiently large number of transmit antennas, we conduct new analysis to simplify the objective function and the corresponding constraints.

A. Optimization Framework

In this work, following [20], [27] we aim to maximize the SSR (i.e., R_s) subject to some constraints on the maximum achievable rates of s_1 and s_2 (i.e., R_{u1} and R_{u2}). Specifically, the focused optimization problem can be written as

$$\mathbf{P1} : \max_{\phi_1, \phi_2, \phi_e, \beta_1, \beta_2} R_s \quad (13)$$

$$\text{s.t. } R_{um} \geq Q_m, \quad m \in \{1, 2\}, \quad (14)$$

$$\phi_1 + \phi_2 + \phi_e = 1, \quad (15)$$

$$0 \leq \beta_m \leq 1, \quad m \in \{1, 2\}, \quad (16)$$

where Q_m denotes the minimum codeword rate required by the m -th legitimate user. We note that the constraint given in (14) can be justified by the fact that secure transmission is only considered when the QoS without security at the m -th user is above a specific threshold [20], [27], [36]. We also note that in the optimization problem given in (13) we have $0 < \phi_m < 1$ and $0 \leq \phi_e < 1$.

Due to the constraint given in (14), there exists a minimum transmit power, denoted by P_{\min} , that guarantees the feasibility of the optimization problem **P1**. In other words, the optimization

problem **P1** is feasible only when $P \geq P_{\min}$. The value of P_{\min} can be determined following the method given in [20] and thus in this work we assume that this feasible condition is always guaranteed.

B. SINR of s_1 and Constraint $R_{um} \geq Q_m$

In this subsection, we present the determined expression (without “min”) for the SINR of s_1 in the following lemma to facilitate solving the optimization problem **P1**, based on which we also transfer the constraint $R_{um} \geq Q_m$ into a specific constraint on ϕ_m .

Lemma 1: In the solution to the optimization problem **P1**, the achieved SINR for s_1 is given by

$$\gamma_{u1} = \frac{\phi_1 P |\mathbf{h}_1 \mathbf{v}_1|^2}{\phi_2 P |\mathbf{h}_1 \mathbf{v}_2|^2 + \sigma_1^2} = \frac{\phi_1 P |\mathbf{h}_2 \mathbf{v}_1|^2}{\phi_2 P |\mathbf{h}_2 \mathbf{v}_2|^2 + \sigma_2^2}. \quad (17)$$

Proof: Following (8), in order to prove this lemma we only have to prove that

$$\frac{\phi_1 P |\mathbf{h}_1 \mathbf{v}_1|^2}{\phi_2 P |\mathbf{h}_1 \mathbf{v}_2|^2 + \sigma_1^2} = \frac{\phi_1 P |\mathbf{h}_2 \mathbf{v}_1|^2}{\phi_2 P |\mathbf{h}_2 \mathbf{v}_2|^2 + \sigma_2^2} \quad (18)$$

is always guaranteed in the solution to the optimization problem **P1**. In what follows, we prove (18) by contradiction. We first assume that

$$\frac{\phi_1 P |\mathbf{h}_1 \mathbf{v}_1|^2}{\phi_2 P |\mathbf{h}_1 \mathbf{v}_2|^2 + \sigma_1^2} > \frac{\phi_1 P |\mathbf{h}_2 \mathbf{v}_1|^2}{\phi_2 P |\mathbf{h}_2 \mathbf{v}_2|^2 + \sigma_2^2} \quad (19)$$

holds in the solution to the optimization problem **P1**. As per (8), following (19) we have

$$\gamma_{u1} = \frac{\phi_1 P |\mathbf{h}_2 \mathbf{v}_1|^2}{\phi_2 P |\mathbf{h}_2 \mathbf{v}_2|^2 + \sigma_2^2}. \quad (20)$$

Based on (2), in this case we can decrease β_1 in order to increase γ_{u1} by slightly increasing the right-hand-side of (19) while decreasing its left-hand-side. This leads to the increase in the SSR (i.e., R_s), which is given in (12), which is contradict to the assumption that (19) is guaranteed in the solution to the optimization problem **P1**. We have a similar argument for the suppose of

$$\frac{\phi_1 P |\mathbf{h}_1 \mathbf{v}_1|^2}{\phi_2 P |\mathbf{h}_1 \mathbf{v}_2|^2 + \sigma_1^2} < \frac{\phi_1 P |\mathbf{h}_2 \mathbf{v}_1|^2}{\phi_2 P |\mathbf{h}_2 \mathbf{v}_2|^2 + \sigma_2^2}, \quad (21)$$

where we can increase the SSR R_s by increasing β_1 . As such, we complete the proof of Lemma 1. ■

Following Lemma 1, for clarity in this work we write the SINR of s_1 as

$$\gamma_{u1} = \frac{\phi_1 P |\mathbf{h}_1 \mathbf{v}_1|^2}{\phi_2 P |\mathbf{h}_1 \mathbf{v}_2|^2 + \sigma_1^2}. \quad (22)$$

Following (7), (9), and Lemma 1, for given β_1 and β_2 , the constraint $R_{um} \geq Q_m$ given in (14) can be rewritten as

$$\phi_1 \geq \frac{2^{Q_1} - 1}{P |\mathbf{h}_1 \mathbf{v}_1|^2} (\phi_2 P |\mathbf{h}_1 \mathbf{v}_2|^2 + \sigma_1^2), \quad (23)$$

and

$$\phi_2 \geq \frac{2^{Q_2} - 1}{P |\mathbf{h}_2 \mathbf{v}_2|^2} \sigma_2^2, \quad (24)$$

respectively.

C. Secrecy Sum Rate with Sufficiently Large N

Considering $N \rightarrow \infty$, we present an approximated but closed-form expression for the SSR (i.e., the objective function in the optimization problem **P1**) in the following theorem.

Proposition 1: As $N \rightarrow \infty$ with $N \gg K$, the SSR given in (12) can be approximated as

$$\begin{aligned} \tilde{R}_s = & \left(1 + \frac{((N-1)\beta_1 + 1)\phi_1 \rho_{u1}}{\phi_2 \rho_{u1} + 1} \right) (1 + ((N-1)\beta_2 + 1)\phi_2 \rho_{u2}) \\ & + \log_2 \left((1 + (1 - \phi_1 - \phi_2)\rho_e)^K \right) - K \log_2(1 + \rho_e), \end{aligned} \quad (25)$$

where $\rho_{u1} = P\delta_1^2/\sigma_1^2$, $\rho_{u2} = P\delta_2^2/\sigma_2^2$, and $\rho_e = P\delta_e^2/\sigma_e^2$ are the average SNRs of the BS-User 1, BS-User 2, and BS-Eve links, respectively.

Proof: The proof is presented in Appendix A. ■

In the remaining of this work, we use the approximated SSR (i.e., \tilde{R}_s) instead of R_s as our objective function, since we focus on the scenario with a sufficiently large number of transmit antennas.

Lemma 2: As $N \rightarrow \infty$, the constraints in (23) and (24) can be rewritten as

$$\phi_1 \geq \frac{2^{Q_1} - 1}{((N-1)\beta_1 + 1)\rho_{u1}} (1 + \phi_2 \rho_{u1}), \quad (26)$$

and

$$\phi_2 \geq \frac{2^{Q_2} - 1}{((N-1)\beta_2 + 1)\rho_{u2}}, \quad (27)$$

respectively.

Proof: The proof of Lemma 2 follows similar arguments as that of Proposition 1 and thus is omitted here. ■

Based on Proposition 1 and Lemma 2, We focus on the optimization problem **P2**, instead of **P1**, in the remaining of this work. Specifically, **P2** is expressed as

$$\mathbf{P2} : \max_{\phi_1, \phi_2, \phi_e, \beta_1, \beta_2} \tilde{R}_s \quad (28)$$

$$\text{s.t. } \phi_1 \geq \frac{(2^{Q_1} - 1)(1 + \phi_2 \rho_{u1})}{((N - 1)\beta_1 + 1)\rho_{u1}}, \quad (29)$$

$$\phi_2 \geq \frac{2^{Q_2} - 1}{((N - 1)\beta_2 + 1)\rho_{u2}}, \quad (30)$$

$$\phi_1 + \phi_2 + \phi_e = 1, \quad (31)$$

$$0 \leq \beta_m \leq 1, \quad m \in \{1, 2\}. \quad (32)$$

We will tackle the optimization problem **P2** in the following section.

IV. POWER ALLOCATION AND BEAMFORMING DESIGN IN MISOME NOMA SYSTEMS

In this section, we first solve **P2** for given values of β_1 and β_2 , where we recast the SSR maximization as a two-level optimization framework that involves a one-dimensional numerical search. Then, we analytically determine the optimal power allocation in the high-SNR regime for fixed β_1 and β_2 . Finally, we provide the method of obtaining the optimal β_1 and β_2 .

A. Optimal Power Allocation for Given β_1 and β_2

For given β_1 and β_2 , the optimization problem **P2** can be rewritten as

$$\begin{aligned} \mathbf{P3} : \max_{\phi_1, \phi_2, \phi_e} \tilde{R}_s(\beta_1, \beta_2) = \max_{\phi_e} & \left\{ \log_2(1 + \phi_e \rho_e)^K \right. \\ & \left. + \max_{\phi_1, \phi_2} \log_2 \left[\left(1 + \frac{c_1 \phi_1}{1 + \phi_2 \rho_{u1}} \right) (1 + c_2 \phi_2) \right] \right\} \\ & - K \log_2(1 + \rho_e) \end{aligned} \quad (33)$$

$$\text{s.t. } \phi_e = 1 - \phi_1 - \phi_2, \quad (34)$$

$$\phi_1 \geq \frac{1}{c_1} (2^{Q_1} - 1)(1 + \phi_2 \rho_{u1}), \quad (35)$$

$$\phi_2 \geq \frac{1}{c_2}(2^{Q_2} - 1), \quad (36)$$

where $\tilde{R}_s(\beta_1, \beta_2)$ denotes \tilde{R}_s given in (28) for given β_1 and β_2 , $c_1 = (1 + (N - 1)\beta_1)\rho_{u1}$, and $c_2 = (1 + (N - 1)\beta_2)\rho_{u2}$. Due to the high complexity of the objective function in the optimization problem **P3**, we solve it in the following two steps. In the first step, for a given power allocation coefficient ϕ_e , we obtain closed-form expressions for the optimal values of the power allocation coefficients ϕ_1 and ϕ_2 , which are functions of ϕ_e . In the second step, we adopt a one-dimensional numerical search to determine the optimal value of ϕ_e , which leads to the optimal power allocation for given β_1 and β_2 .

In the first step of solving the optimization problem **P3**, we tackle the following optimization problem for a given ϕ_e :

$$\mathbf{P4} : \max_{\phi_1, \phi_2} F(\phi_1, \phi_2) \quad (37)$$

$$\text{s.t. } \phi_1 + \phi_2 = 1 - \phi_e, \quad (38)$$

$$\phi_1 \geq \frac{1}{c_1}(2^{Q_1} - 1)(1 + \phi_2\rho_{u1}), \quad (39)$$

$$\phi_2 \geq \frac{1}{c_2}(2^{Q_2} - 1), \quad (40)$$

where

$$F(\phi_1, \phi_2) = \log_2 \left[\left(1 + \frac{c_1\phi_1}{1 + \phi_2\rho_{u1}} \right) (1 + c_2\phi_2) \right]. \quad (41)$$

We note that the feasible range of ϕ_e is $0 \leq \phi_e \leq \frac{P - P_{min}}{P}$, where we recall that P_{min} is the minimum transmit power that guarantees the QoS constraints at the two legitimate users. We also note that due to the constraint given in (38) the only parameter to optimize in **P4** is ϕ_1 or ϕ_2 . Here, we take ϕ_2 as the parameter to optimize. Then, we have the following lemma to facilitate solving the optimization problem **P4**.

Lemma 3: For $\phi_1 + \phi_2 = 1 - \phi_e$, the objective function in **P4**, i.e., $F(\phi_1, \phi_2)$ given in (41), is a concave function of ϕ_2 .

Proof: The proof is presented in Appendix B. ■

Following Lemma 3, the solution to the optimization problem **P4** is given in the following theorem.

Theorem 1: For a given feasible ϕ_e , the optimal values of ϕ_1 and ϕ_2 for the optimization problem P4 are derived as functions of ϕ_e , given by

$$\phi_2^\dagger(\phi_e) = \begin{cases} \mu_0, & \text{when } \mu_1 \leq \mu_0 \leq \mu_2, \\ \mu_1, & \text{when } \mu_0 < \mu_1, \\ \mu_2, & \text{when } \mu_0 > \mu_2, \end{cases} \quad (42)$$

$$\phi_1^\dagger(\phi_e) = 1 - \phi_e - \phi_2^\dagger(\phi_e), \quad (43)$$

where

$$\mu_0 = \frac{\sqrt{c_2^2 c_3^2 - c_2 c_3 \rho_{u1} c_4 - c_2 c_3}}{c_2 c_3 \rho_{u1}}, \quad (44)$$

$$\mu_1 = \frac{1}{c_2} (2^{Q_2} - 1), \quad (45)$$

$$\mu_2 = \frac{1 - \phi_e - \frac{1}{c_1} (2^{Q_1} - 1)}{1 + \frac{(2^{Q_1} - 1)}{(N-1)\beta_1 + 1}}. \quad (46)$$

Proof: Based on Lemma 3, the optimal value of ϕ_2 that maximizes the objective function in P4 without considering the constraints given in (39) and (40) is the one that guarantees $\frac{\partial F(\phi_1, \phi_2)}{\partial \phi_2} = 0$ (i.e., $G(\phi_2)' = 0$ in (75) of Appendix B), which is given by (following Lemma 3 again)

$$\mu_0 = \frac{\sqrt{c_2^2 c_3^2 - c_2 c_3 \rho_{u1} c_4 - c_2 c_3}}{c_2 c_3 \rho_{u1}}. \quad (47)$$

Substituting (38) into (39), the constraints given in (39) and (40) can be rewritten as the constraints on ϕ_2 , given by

$$\mu_1 \leq \phi_2 \leq \mu_2. \quad (48)$$

If μ_0 satisfies the constraints given in (48), we can directly conclude $\phi_2^\dagger(\phi_e) = \mu_0$. Otherwise, we have the following two cases. For $\mu_0 < \mu_1$, we have $\phi_2^\dagger(\phi_e) = \mu_1$. This is due to the fact that, as we proved in Lemma 3, the objective function $F(\phi_1, \phi_2)$ is a concave function of ϕ_2 and μ_0 is the value of ϕ_2 that maximizes $F(\phi_1, \phi_2)$, which leads to the fact that when $\mu_0 < \mu_1$ the objective function $F(\phi_1, \phi_2)$ monotonically decreases with ϕ_2 for $\mu_1 \leq \phi_2 \leq \mu_2$. Following a similar argument, we have $\phi_2^\dagger(\phi_e) = \mu_2$ when $\mu_0 > \mu_2$. This completes the proof of Theorem 1. ■

Following Theorem 1, in the second step of solving the optimization problem **P3** we have to solve a univariate optimization problem with respect to ϕ_e , which is given by

$$\mathbf{P5} : \max_{0 \leq \phi_e \leq (P - P_{min})/P} \left[\log_2 (1 + \phi_e \rho_e)^K + F(\phi_1^*(\phi_e), \phi_2^*(\phi_e)) - K \log_2(1 + \rho_e) \right]. \quad (49)$$

We note that the optimization problem **P5** is identical to **P3**. For the optimization problem **P5**, we can perform a one-dimensional numerical search over $0 \leq \phi_e \leq (P - P_{min})/P$ to determine the optimal value of ϕ_e , i.e., ϕ_e^* . Then, substituting ϕ_e^* into Theorem 1 we can obtain the optimal values of ϕ_1 and ϕ_2 , which are denoted by ϕ_1^* and ϕ_2^* , respectively. So far, we have solved the optimization problem **P3** with the aid of a one-dimensional numerical search, which determines the optimal power allocation strategy for given β_1 and β_2 . In order to reduce the complexity of determining the optimal power allocation and provide some insights based on analysis, in the following subsection we focus on analytically determining the optimal power allocation in the high-SNR regime.

B. Optimal Power Allocation in High-SNR Regime

In the high-SNR regime, i.e., as $\rho_{u1} \rightarrow \infty$ and $\rho_{u2} \rightarrow \infty$, following (70), $R_{u1} + R_{u2}$ can be further approximated as

$$\begin{aligned} R_{u1} + R_{u2} &= \log_2 (1 + \phi_2 N \beta_2 \rho_{u2} + \phi_2 (1 - \beta_2) \rho_{u2}) \\ &\quad + \log_2 \left(1 + \frac{\phi_1 \rho_{u1} + \phi_1 (N - 1) \beta_1 \rho_{u1}}{\phi_2 \rho_{u1} + 1} \right) \\ &= \log_2 (c_2 \phi_2) + \log_2 \left(\frac{\phi_1 ((N - 1) \beta_1 + 1) \rho_{u1}}{\phi_2 \rho_{u1}} \right) \\ &= \log_2 (((N - 1) \beta_1 + 1) c_2 \phi_1). \end{aligned} \quad (50)$$

Noting $\phi_1 + \phi_2 + \phi_e = 1$ and following (50), for given β_1 and β_2 the optimization problem **P2** can be rewritten as

$$\mathbf{P6} : \max_{\phi_1, \phi_2} \tilde{R}_s(\beta_1, \beta_2) = \max_{\phi_1, \phi_2} \left[\log_2 \left(\phi_1 (1 + (1 - \phi_1 - \phi_2) \rho_e)^K \right) + \log_2 (((N - 1) \beta_1 + 1) c_2) - K \log_2(1 + \rho_e) \right] \quad (51)$$

$$\text{s.t. } \phi_1 \geq \frac{1}{c_1} (2^{Q_1} - 1) (1 + \phi_2 \rho_{u1}), \quad (52)$$

$$\phi_2 \geq \frac{1}{c_2}(2^{Q_2} - 1). \quad (53)$$

The solution to the optimization problem **P6** is presented in the following theorem.

Theorem 2: In the high SNR regime, i.e., as $\rho_{u1} \rightarrow \infty$ and $\rho_{u2} \rightarrow \infty$, the optimal power allocation coefficients, which are solutions to the optimization problem **P6**, are derived as

$$\phi_1^* = \begin{cases} \frac{1+\rho_e-\gamma_1\rho_e}{(K+1)\rho_e}, & \text{when } \gamma_0 \leq \frac{1+\rho_e-\gamma_1\rho_e}{(K+1)\rho_e} \leq 1 - \gamma_1, \\ 1 - \gamma_1, & \text{when } \frac{1+\rho_e-\gamma_1\rho_e}{(K+1)\rho_e} > 1 - \gamma_1, \\ \gamma_0, & \text{when } \frac{1+\rho_e-\gamma_1\rho_e}{(K+1)\rho_e} < \gamma_0, \end{cases} \quad (54)$$

$$\phi_2^* = \gamma_1, \quad (55)$$

$$\phi_e^* = 1 - \phi_1^* - \phi_2^*, \quad (56)$$

where $\gamma_0 = \frac{1}{c_1}(2^{Q_1} - 1)(1 + \gamma_1\rho_{u1})$ and $\gamma_1 = \mu_1$.

Proof: As per (51), the objective function in **P6**, i.e., the SSR $\tilde{R}_s(\beta_1, \beta_2)$, monotonically decreases with ϕ_2 . Noting the constraints given in (52) and (53), we conclude that the optimal value of ϕ_2 is the one that guarantees the equality in (53), since decreasing ϕ_2 makes the constraint given in (52) be guaranteed more easily. After obtaining the optimal value of ϕ_2 (i.e., $\phi_2^* = \gamma_1$), the optimization problem **P6** can be rewritten as

$$\mathbf{P7} : \max_{\phi_1} \tilde{R}_s(\beta_1, \beta_2) = \max_{\phi_1} \log_2 \left[\left(\phi_1 (1 + (1 - \phi_1 - \gamma_1)\rho_e)^K \right) + \log_2(((N - 1)\beta_1 + 1)c_2) - K \log_2(1 + \rho_e) \right] \quad (57)$$

$$\text{s.t. } \gamma_0 \leq \phi_1 \leq 1 - \gamma_1, \quad (58)$$

where the constraint given in (58) comes from (52), (53), and the consideration of $\phi_1 + \phi_2 + \phi_e = 1$ and $0 \leq \phi_e$.

In the following, we first maximize the objective function in **P7** given in (57) without considering the constraint of (58), which is presented in the following lemma.

Lemma 4: The term of $\phi_1 (1 + (1 - \phi_1 - \gamma_1)\rho_e)^K$ in the objective function of **P7** (i.e., the first term given in (57)) is maximized over ϕ_1 when $\phi_1 = \frac{1+\rho_e-\gamma_1\rho_e}{(K+1)\rho_e}$.

Proof: The proof is presented in Appendix C. ■

Based on (57), we find that the second and third terms in the objective function of **P7** are not functions of ϕ_1 . Since $\log x$ is an increasing function of x , the value of $\log x$ is maximized when x is maximized. As such, in order to maximize the objective function in **P7** (i.e., (57)) without considering the constraint of (58), following Lemma 4, we have $\phi_1 = \frac{1+\rho_e-\gamma_1\rho_e}{(K+1)\rho_e}$.

Now, we consider the constraint of (58) in **P7**. Specifically, if $\frac{1+\rho_e-\gamma_1\rho_e}{(K+1)\rho_e}$ satisfies the constraints given in (58), we can directly conclude $\phi_1^* = \frac{1+\rho_e-\gamma_1\rho_e}{(K+1)\rho_e}$. Otherwise, we have the following two cases, which directly follow from the proof of Lemma 4. Specifically, if $\frac{1+\rho_e-\gamma_1\rho_e}{(K+1)\rho_e} < 1 - \gamma_1$, we have $\phi_1^* = 1 - \gamma_1$. Otherwise, we have $\phi_1^* = \gamma_0$. Finally, we can obtain the optimal power allocation coefficient for AN as $\phi_e^* = 1 - \phi_1^* - \phi_2^*$. This completes the proof of Theorem 2. ■

Following Theorem 2, we note that ϕ_2^*P is a fixed value regardless of the total transmit power P in the high-SNR regime, which is given by

$$\phi_2^*P = \frac{\sigma_2^2}{(1 + (N - 1)\beta_2)\delta_2^2}(2^{Q_2} - 1). \quad (59)$$

This indicates that for a downlink MISOME NOMA system, the optimal power allocation policy for maximizing the SSR is to use a fixed transmit power to User 2 in order to guarantee the equality in its QoS constraint and then allocate the remaining transmit power ($P - P_{\min}$) to User 1 or transmitting AN signals. This is different from the conclusion drawn in [20], which is that the extra transmit power is still allocated to User 2. As per (59), we also note that the transmit power allocated to User 2 (i.e., ϕ_2^*P) decreases with N , which is not a function of K .

Following Theorem 2, for $\gamma_0 \leq \frac{1+\rho_e-\gamma_1\rho_e}{(K+1)\rho_e} \leq 1 - \gamma_1$, ϕ_e^* increases with K or ρ_e , while ϕ_1^* decreases with K or ρ_e . This indicates that for a fixed total transmit power, we need to allocate more transmit power to AN when Eve's channel quality becomes higher.

For $\frac{1+\rho_e-\gamma_1\rho_e}{(K+1)\rho_e} > 1 - \gamma_1$, we have $\phi_e^* = 0$ as per Theorem 2, which indicates that under some specific conditions it is not necessary to transmit AN. We note that the value of $\frac{1+\rho_e-\gamma_1\rho_e}{(K+1)\rho_e}$ increases when K or ρ_e decreases. This indicates that as Eve's channel quality becomes lower the probability of the BS having to transmit AN decreases.

Following Theorem 2, for $\gamma_0 > \frac{1+\rho_e-\gamma_1\rho_e}{(K+1)\rho_e}$ in the optimal power allocation we have that the transmit power allocated to User 1 and User 2 only guarantees the equality in their QoS

constraints and then all the remaining transmit power is allocated to AN. The probability of this case increases with K and ρ_e , for which Eve is a very strong eavesdropper.

C. Optimization of Beamforming Parameters β_1 and β_2

So far, we have presented the optimization of the power allocation coefficients for given beamforming parameters β_1 and β_2 . In this subsection, we discuss the optimization framework of β_1 and β_2 .

We note that Lemma 1 determines a one-to-one relationship between β_1 and β_2 . Specifically, following (8) and considering $N \rightarrow \infty$, we have

$$\begin{aligned}\gamma_{u1}^1(\beta_1, \beta_2) &\triangleq \frac{\phi_1 P |\mathbf{h}_1 \mathbf{v}_1|^2}{\phi_2 P |\mathbf{h}_1 \mathbf{v}_2|^2 + \sigma_1^2} \\ &= \frac{\phi_1 (N\beta_1 + 1) \rho_{u1} - \phi_1 \beta_1 \rho_{u1}}{\phi_2 \rho_{u1} + 1} \\ &\approx \frac{\phi_1 (N\beta_1 + 1) \rho_{u1}}{\phi_2 \rho_{u1} + 1},\end{aligned}\tag{60}$$

$$\begin{aligned}\gamma_{u1}^2(\beta_1, \beta_2) &\triangleq \frac{\phi_1 P |\mathbf{h}_2 \mathbf{v}_1|^2}{\phi_2 P |\mathbf{h}_2 \mathbf{v}_2|^2 + \sigma_2^2} \\ &= \frac{\phi_1 N (1 - \beta_1) \rho_{u2} + \phi_1 \beta_1 \rho_{u2}}{1 + \phi_2 (1 + N\beta_2) \rho_{u2}} \\ &\approx \frac{\phi_1 N (1 - \beta_1) \rho_{u2}}{1 + \phi_2 (1 + N\beta_2) \rho_{u2}}.\end{aligned}\tag{61}$$

Then, by setting $\gamma_{u1}^1(\beta_1, \beta_2) = \gamma_{u1}^2(\beta_1, \beta_2)$ as per Lemma 1, we can obtain the one-to-one relationship between β_1 and β_2 . Thus, the optimization problem **P2** can be rewritten as

$$\mathbf{P8} : \max_{\beta_1, \beta_2} \tilde{R}_s^*(\beta_1, \beta_2)\tag{62}$$

$$\text{s.t. } \frac{\phi_1^* (N\beta_1 + 1) \rho_{u1}}{\phi_2^* \rho_{u1} + 1} = \frac{\phi_1^* N (1 - \beta_1) \rho_{u2}}{1 + \phi_2^* (1 + N\beta_2) \rho_{u2}},\tag{63}$$

$$0 \leq \beta_m \leq 1, \quad m \in \{1, 2\},\tag{64}$$

where $\tilde{R}_s^*(\beta_1, \beta_2)$ is the maximum SSR achieved by the optimal power allocation for fixed β_1 and β_2 .

As detailed in Section IV-A, the optimal power allocation for given β_1 and β_2 cannot be analytically determined with arbitrary SNRs, for which a one-dimensional numerical search is involved. As such, in the arbitrary SNR regime the optimization problem **P8** cannot be

analytically solved. We note that a three-dimensional numerical search should be adopted to solve the optimization problem **P8**, since the one-to-one relationship between β_1 and β_2 given in (63) depends on the optimal power allocation obtained from the one-dimensional numerical search. In order to reduce the complexity of solving optimization problem **P8** with a three-dimensional numerical search method, we next discuss how to efficiently solve it in the high-SNR regime.

In the high-SNR regime, following Lemma 1, (60), and (61), we have

$$\begin{aligned} \frac{(N\beta_1 + 1)\phi_1\rho_{u1}}{\phi_2\rho_{u1} + 1} &= \frac{N\phi_1(1 - \beta_1)\rho_{u2}}{1 + (1 + N\beta_2)\phi_2\rho_{u2}} \\ \Rightarrow \frac{(N\beta_1 + 1)\phi_1}{\phi_2} &= \frac{N\phi_1(1 - \beta_1)}{\phi_2(1 + N\beta_2)} \\ \Rightarrow \beta_2 &= \frac{1}{1 + N\beta_1}(1 - \beta_1). \end{aligned} \quad (65)$$

Then, the optimization problem **P8** can be rewritten as

$$\mathbf{P9} : \max_{\beta_1, \beta_2} \tilde{R}_s^*(\beta_1, \beta_2) \quad (66)$$

$$\text{s.t. } \beta_2 = \frac{1}{1 + N\beta_1}(1 - \beta_1), \quad (67)$$

$$0 \leq \beta_m \leq 1, \quad m \in \{1, 2\}, \quad (68)$$

which is identical to the optimization problem of **P2** in the high-SNR regime. We note that the optimization problem **P9** can be efficiently solved by a one-dimensional numerical search method, since as detailed in Theorem 2 the optimal power allocation can be determined in closed-form expressions in the high-SNR regime, in which the one-to-one relationship given in (67) is also independent of the power allocation coefficients. As confirmed in our following numerical results, the achieved solution to **P9** is very close to the solution to **P8** and their resultant maximum SSRs are very similar to each other. This indicates that our proposed beamforming design can be optimized efficiently by a one-dimensional numerical search.

V. NUMERICAL RESULTS

In this section, we provide numerical results to examine the secrecy performances of the proposed NOMA-HB-AN scheme relative to two benchmark schemes. The first benchmark scheme is named as the NOMA-HB scheme, in which the beamforming design is the same

as the proposed NOMA-HB-AN scheme, but no AN is transmitted by the BS. The second benchmark scheme is named as the NOMA- \mathbf{h}_2 -AN scheme, which is proposed in [26]. In the NOMA- \mathbf{h}_2 -AN scheme, the beamforming vectors are set such as $\mathbf{v}_1 = \mathbf{v}_2 = \mathbf{h}_2/\|\mathbf{h}_2\|$ and the AN signals are transmitted by the BS simultaneously. In this section, we set $\rho_{su} = \rho_{su2} = 1.2\rho_{su1}$.

In Fig. 2, we plot the maximum SSRs achieved by the NOMA-HB-AN, NOMA-HB, and NOMA- \mathbf{h}_2 -AN schemes with the optimal power allocation versus the number of antennas at base station (i.e., N). In this figure, the simulated SSR of the proposed NOMA-HB-AN scheme is obtained by performing Monte Carlo simulations over 10^5 different channel realizations. We first observe that the analytical curve of the NOMA-HB-AN scheme accurately match the simulated one for different values of N , which confirms the high accuracy of the approximation adopted in our Proposition 1. In this figure, we also observe that the proposed NOMA-HB-AN scheme outperforms the NOMA- \mathbf{h}_2 -AN scheme. This demonstrates the effectiveness of the proposed beamforming design. We note that in this figure we set $\beta_1 = 0.05$ and $\beta_2 = 0.9$, which means that the performance gain of the proposed scheme over the NOMA- \mathbf{h}_2 -AN scheme can be further improved by jointly optimizing β_1 and β_2 . Furthermore, we observe that the proposed NOMA-HB-AN scheme outperforms the NOMA-HB scheme in terms of achieving a significantly higher maximum SSR, which shows the benefits of using AN-aided transmission schemes in enhancing physical layer security of NOMA systems. Finally, as expected we observe that the SSR increases with N .

In Fig. 3, we plot the maximum SSRs of the NOMA-HB-AN, NOMA-HB, and NOMA- \mathbf{h}_2 -AN schemes versus the number of antennas at Eve (i.e., K). In this figure, the power allocation coefficients together with the values of β_1 and β_2 in the NOMA-HB-AN and NOMA-HB schemes have been optimized based on our conducted analysis in Section III and Section IV (e.g., Proposition 1, Theorem 1). The power allocation coefficients in the NOMA- \mathbf{h}_2 -AN scheme have been optimized based on the analysis presented in [26]. Again, in this figure we first observe that the proposed NOMA-HB-AN scheme significantly outperforms the two benchmark schemes, which again demonstrates the superiority of the proposed beamforming design. As expected, we observe that the achieved maximum SSRs decrease with K . We further observe

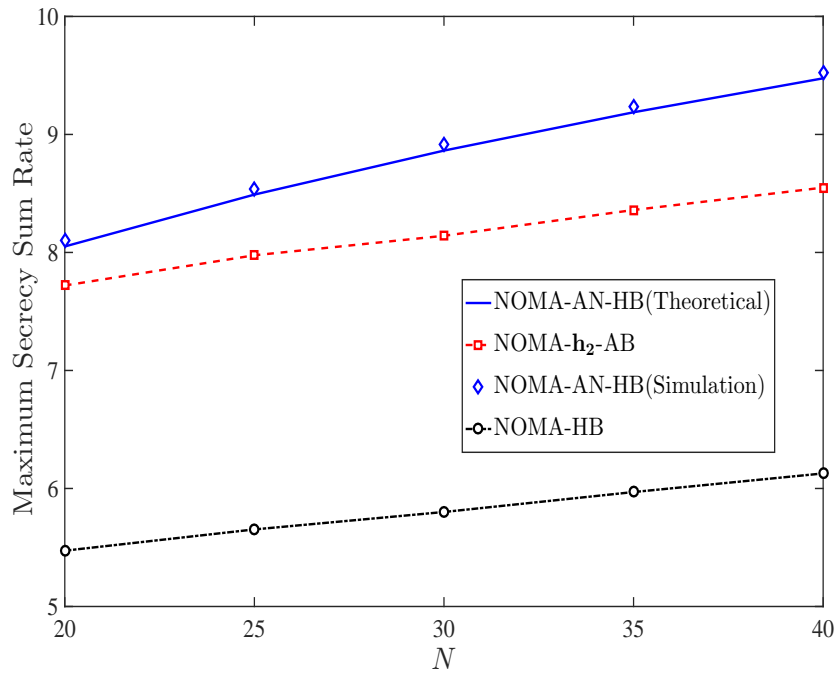


Fig. 2. Maximum secrecy sum rate achieved by three different schemes versus the number of antennas at the BS N , where $\rho_{su} = 20$ dB, $\rho_e = 10$ dB, $K = 2$, $Q_1 = 5$ BPCU, $Q_2 = 5.5$ BPCU, $\beta_1 = 0.05$, and $\beta_2 = 0.9$.

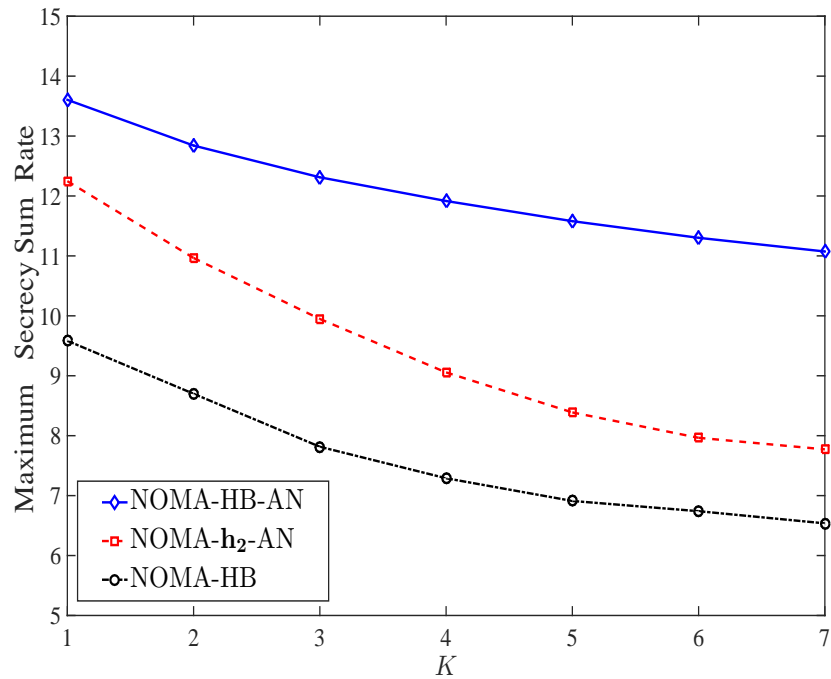


Fig. 3. Maximum secrecy sum rate achieved by three different schemes versus the number of antennas at Eve K , where $Q_1 = 5$ BPCU, $Q_2 = 5.5$ BPCU, $\rho_{su} = 20$ dB, $\rho_e = 0$ dB, and $N = 40$.

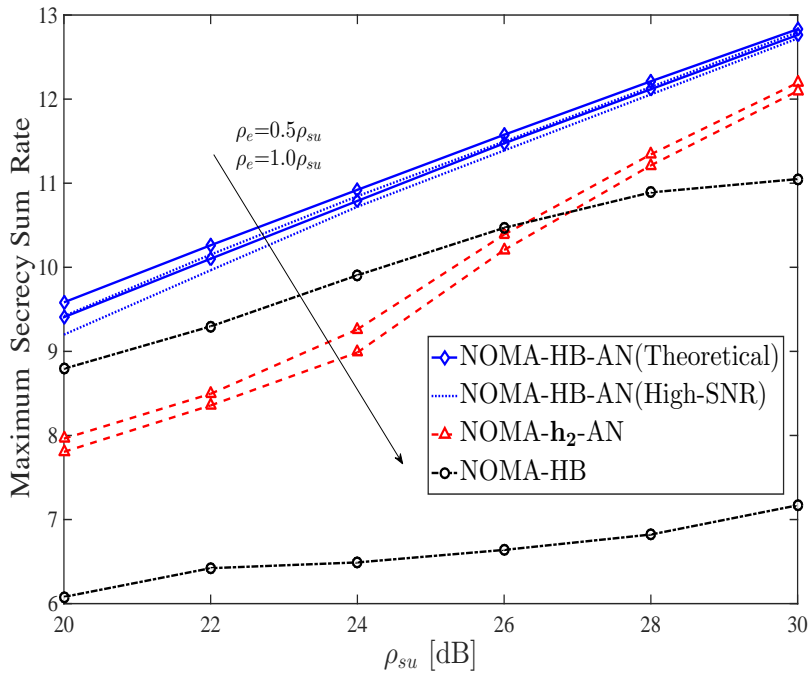


Fig. 4. Maximum secrecy sum rate achieved by three different schemes versus the average SNR ρ_{su} with $\rho_e = 0.5\rho_{su}$ and $\rho_e = \rho_{su}$, where $N = 30$, $Q_1 = 5$ BPCU, $Q_2 = 5.5$ BPCU, and $K = 2$.

that the performance gain of the proposed scheme over the NOMA-h₂-AN scheme increases with K . This indicates that the advantage of the proposed scheme relative to the NOMA-h₂-AN scheme becomes more dominant as K increases, which shows the effectiveness of the proposed beamforming design increases with K .

In Fig. 4, we plot the maximum SSRs of the NOMA-HB-AN, NOMA-HB, and NOMA-h₂-AN schemes versus the average SNR of the legitimate channels. We recall that we have set $\rho_{su} = \rho_{su2} = 1.2\rho_{su1}$. In this figure, we first observe that, for the proposed NOMA-HB-AN scheme, the results achieved in the high-SNR regime (i.e., dashed curves) are very close to the exact results achieved for arbitrary SNRs (solid curves). We note that, in the high-SNR regime, the power allocation and the values of β_1 and β_2 are optimized by a one-dimensional numerical search with the aid of our Theorem 2, while, for arbitrary SNRs, the power allocation, β_1 , and β_2 have to be optimized by a three-dimensional numerical search with the aid of our Theorem 1. As such, this observation demonstrates the usefulness of the asymptotic analysis in the high-SNR regime, i.e., the optimal power allocation together with the optimal β_1 and β_2 can be accurately

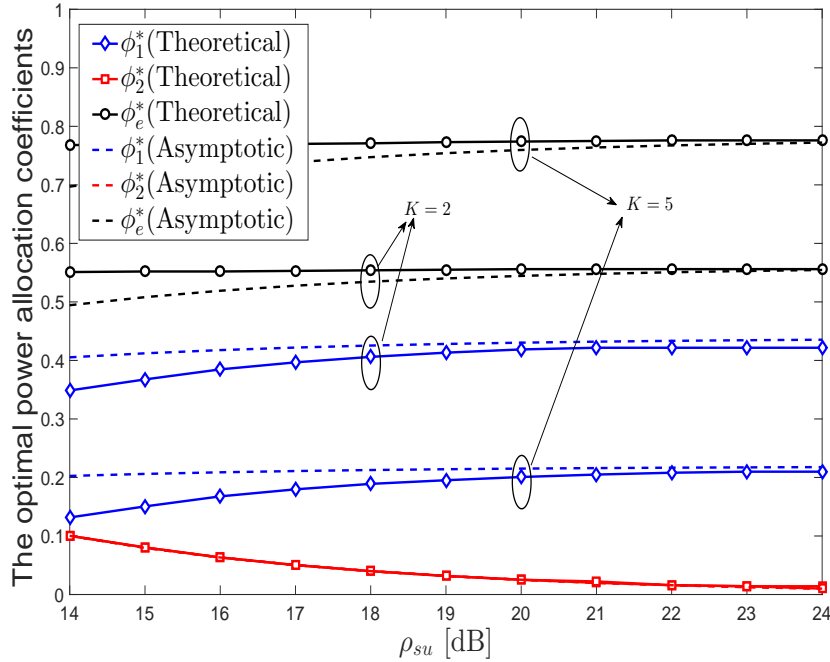


Fig. 5. The optimal power allocation coefficients versus the average SNR of the legitimate users’ channels ρ_{su} with $K = 2$ and $K = 5$, where $\rho_e = 15\text{dB}$, $Q_1 = 2$ BPCU, $Q_2 = 6$ BPCU, and $N = 20$.

approximated by those achieved in the high-SNR regime, which can significantly reduce the complexity of optimally designing the beamforming vectors and power allocation. As expected, we also observe that the proposed scheme outperforms the two benchmark schemes. Interestingly, we further observe that the NOMA-HB scheme can outperform the NOMA-h₂-AN scheme for $\rho_e = 0.5\rho_{su}$ and a relatively small ρ_{su} . This is due to the following two facts. First, the benefits of using AN decreases as ρ_e decreases (i.e., Eve moves further from the BS). Second, the proposed hybrid beamforming design brings more benefits than using AN in the specific scenario. This observation again demonstrates the effectiveness of the our proposed novel beamforming design. Finally, in this figure we observe that when ρ_e increases from $\rho_e = 0.5\rho_{su}$ to $\rho_e = \rho_{su}$, the secrecy performance of both the proposed NOMA-HB-AN scheme and the NOMA-h₂-AN scheme only slightly decreases, but the NOMA-HB scheme suffers from a significant SSR degradation. This observation again shows the benefits of using the AN-aided transmission strategies to enhance physical layer security of NOMA systems.

In Fig. 5, we plot the optimal power allocation coefficients of the NOMA-HB-AN scheme

versus the average SNR ρ_{su} with $K = 2$ and $K = 5$. In this figure, we first observe that the power allocation coefficients achieved for arbitrary SNRs approach those achieved for high SNRs when ρ_{su} increases, which again demonstrates the correctness and usefulness of our conducted asymptotic analysis in the high-SNR regime. Moreover, we observe that the the power allocation coefficients for User 1 and AN increase with ρ_{su} , while the power allocation coefficient for User 2 decreases when ρ_{su} increases. This observation demonstrates that as the transmit power increases the remaining power (i.e., $P - P_{\min}$) is more likely allocated to either User 1 or used for transmitting AN signals in order to achieve the maximum SSR. We further observe that the power allocation coefficient ϕ_e^* increases with the number of antennas at Eve (i.e., K), illustrating the benefits of transmitting more AN signal to prevent eavesdropping attacks when the Eve's channel quality increases. Finally, we observe that the power allocation coefficient ϕ_2^* is independent of the number of antennas at Eve. These two observations can be explained by our analysis in Section IV-B, i.e., Theorem 2 and its followed discussions.

VI. CONCLUSION

In this work, we developed a novel beamforming design with the optimal power allocation to enhance physical layer security of a NOMA system. Specifically, we adopted two governing scalars to determine the beamforming vector, which can balance the SNR or SINR between the weak and strong users in the considered NOMA system. In order to demonstrate the benefits of our proposed beamforming design, we determined the optimal power allocation among information and AN signals by focusing on the asymptotic scenario with a large number of transmit antennas but an arbitrary SNR, based on which we also optimized the two governing scalars in the proposed beamforming design in order to maximize the SSR. In addition, we obtained an efficient solution to the optimization of the power allocation coefficients and the governing scalars in the high SNR regime, which is shown as a generic and near-optimal strategy. Our examination confirmed that our proposed NOMA-HB-AN scheme can significantly outperform the existing benchmark schemes, i.e., the NOMA-HB and NOMA-h₂-AN schemes.

APPENDIX A

PROOF OF PROPOSITION 1

By substituting (7), (9), (10), and (11) into (13), R_s can be rewritten as

$$\begin{aligned}
R_s &= R_{u1} + R_{u2} - R_{e1} - R_{e2} \\
&= \log_2 \left(1 + \frac{\phi_2 P |\mathbf{h}_2 \mathbf{v}_2|^2}{\sigma_2^2} \right) + \log_2 \left(1 + \frac{\phi_1 P |\mathbf{h}_1 \mathbf{v}_1|^2}{\phi_2 P |\mathbf{h}_1 \mathbf{v}_2|^2 + \sigma_1^2} \right) \\
&\quad - \log_2 \det \left(\sigma_e^2 \mathbf{I}_K + \frac{\phi_2 P \mathbf{H}_e \mathbf{v}_2 (\mathbf{H}_e \mathbf{v}_2)^H}{\frac{\phi_e P}{N-2} \mathbf{H}_e \mathbf{V}_N (\mathbf{H}_e \mathbf{V}_N)^H + \sigma_e^2 \mathbf{I}_K} \right) \\
&\quad - \log_2 \det \left(\sigma_e^2 \mathbf{I}_K + \frac{\phi_1 P \mathbf{H}_e \mathbf{v}_1 (\mathbf{H}_e \mathbf{v}_1)^H}{P \phi_2 \mathbf{H}_e \mathbf{v}_2 (\mathbf{H}_e \mathbf{v}_2)^H + \frac{\phi_e P}{N-2} \mathbf{H}_e \mathbf{V}_N (\mathbf{H}_e \mathbf{V}_N)^H + \sigma_e^2 \mathbf{I}_K} \right). \tag{69}
\end{aligned}$$

To proceed, according to the law of large numbers, we have that, as $N \rightarrow \infty$, the value of $|\mathbf{h}_i \hat{\mathbf{h}}_i|^2$ converges in probability to $N\delta_i^2$, the value of both $|\mathbf{h}_i \hat{\mathbf{e}}|^2$ and $|\mathbf{h}_i \hat{\mathbf{h}}_j|^2$ with $i \neq j$ converges in probability to δ_i^2 , and the value of both $\|\sqrt{\beta_1} \hat{\mathbf{h}}_1 + \sqrt{(1-\beta_1)} \hat{\mathbf{h}}_2\|$ and $\|\sqrt{\beta_2} \hat{\mathbf{h}}_2 + \sqrt{(1-\beta_2)} \hat{\mathbf{e}}\|$ converges in probability to 1. Then we have

$$\begin{aligned}
R_{u1} + R_{u2} &= \log_2 \left(1 + \frac{\phi_2 P |\mathbf{h}_2 \mathbf{v}_2|^2}{\sigma_2^2} \right) + \log_2 \left(1 + \frac{\phi_1 P |\mathbf{h}_1 \mathbf{v}_1|^2}{\phi_2 P |\mathbf{h}_1 \mathbf{v}_2|^2 + \sigma_1^2} \right) \\
&\approx \log_2 (1 + \phi_2 ((N-1)\beta_2 + 1)\rho_{u2}) + \log_2 \left(1 + \frac{\phi_1 ((N-1)\beta_1 + 1)\rho_{u1}}{\phi_2 \rho_{u1} + 1} \right). \tag{70}
\end{aligned}$$

For the term $R_{e1} + R_{e2}$ in (13), we have

$$\begin{aligned}
&R_{e1} + R_{e2} \\
&= \log_2 \det \left(\mathbf{I}_K + \frac{\phi_2 \pi_e \mathbf{H}_e \mathbf{v}_2 (\mathbf{H}_e \mathbf{v}_2)^H}{\frac{\phi_e \pi_e}{N-2} \mathbf{H}_e \mathbf{V}_N (\mathbf{H}_e \mathbf{V}_N)^H + \mathbf{I}_K} \right) \\
&\quad + \log_2 \det \left(\mathbf{I}_K + \frac{\phi_1 \pi_e \mathbf{H}_e \mathbf{v}_1 (\mathbf{H}_e \mathbf{v}_1)^H}{\phi_2 \pi_e \mathbf{H}_e \mathbf{v}_2 (\mathbf{H}_e \mathbf{v}_2)^H + \frac{\phi_e \pi_e}{N-2} \mathbf{H}_e \mathbf{V}_N (\mathbf{H}_e \mathbf{V}_N)^H + \mathbf{I}_K} \right) \\
&= \log_2 \det \left(\mathbf{I}_K + \phi_1 \pi_e \mathbf{H}_e \mathbf{v}_1 (\mathbf{H}_e \mathbf{v}_1)^H + \phi_2 \pi_e \mathbf{H}_e \mathbf{v}_2 (\mathbf{H}_e \mathbf{v}_2)^H + \frac{\phi_e \pi_e}{N-2} \mathbf{H}_e \mathbf{V}_N (\mathbf{H}_e \mathbf{V}_N)^H \right) \\
&\quad - \log_2 \det \left(\mathbf{I}_K + \frac{\phi_e \pi_e}{N-2} \mathbf{H}_e \mathbf{V}_N (\mathbf{H}_e \mathbf{V}_N)^H \right). \tag{71}
\end{aligned}$$

In order to simplify (69), we present the following lemma (i.e., Lemma 5) to facilitate our proof.

Lemma 5: As $N \rightarrow \infty$ with $N \gg K$, we have

$$\begin{aligned}
 & \det \left(\mathbf{I}_K + \phi_1 \pi_e \mathbf{H}_e \mathbf{v}_1 (\mathbf{H}_e \mathbf{v}_1)^H + \phi_2 \pi_e \mathbf{H}_e \mathbf{v}_2 (\mathbf{H}_e \mathbf{v}_2)^H + \frac{\phi_e \pi_e}{N-2} \mathbf{H}_e \mathbf{V}_N (\mathbf{H}_e \mathbf{V}_N)^H \right) \\
 & \leq \prod_{k=1}^K \left(1 + \phi_1 \pi_e [\mathbf{H}_e \mathbf{v}_1 (\mathbf{H}_e \mathbf{v}_1)^H]_{kk} + \phi_2 \pi_e [\mathbf{H}_e \mathbf{v}_2 (\mathbf{H}_e \mathbf{v}_2)^H]_{kk} + \frac{(1-\phi_1-\phi_2)\pi_e}{N-2} [\mathbf{H}_e \mathbf{V}_N (\mathbf{H}_e \mathbf{V}_N)^H]_{kk} \right) \\
 & \approx (1 + \phi_1 \rho_e + \phi_2 \rho_e + (1 - \phi_1 - \phi_2) \rho_e)^K \\
 & = (1 + \rho_e)^K,
 \end{aligned} \tag{72}$$

and

$$\det \left(\mathbf{I}_K + \frac{\phi_e \pi_e}{N-2} \mathbf{H}_e \mathbf{V}_N (\mathbf{H}_e \mathbf{V}_N)^H \right) \approx \prod_{k=1}^K \left(1 + \frac{\phi_e \pi_e}{N-2} [\mathbf{H}_e \mathbf{V}_N (\mathbf{H}_e \mathbf{V}_N)^H]_{kk} \right) = (1 + \phi_e \rho_e)^K. \tag{73}$$

The proof of Lemma 5 is given in [34] and thus it is omitted here. Based on (70), (71), and Lemma 5, we can obtain (25), which completes the proof of Proposition 1.

APPENDIX B

PROOF OF LEMMA 3

Substituting (39) into (37), we have

$$F(\phi_1, \phi_2) = \log_2 \left(1 + \frac{c_1(1 - \phi_2 - \phi_e)}{1 + \phi_2 \rho_{u1}} \right) (1 + c_2 \phi_2) \triangleq G(\phi_2). \tag{74}$$

From (74), we can obtain the first derivative of $G(\phi_2)$ with respect to ϕ_2 as $G(\phi_2)'$, which is give by

$$G(\phi_2)' = \frac{\partial G(\phi_2)}{\partial \phi_2} = \frac{1}{\ln(2)} \frac{c_2 c_3 \rho_{u1} \phi_2^2 + 2c_2 c_3 \phi_2 + c_4}{(1 + \phi_2 \rho_{u1})^2}, \tag{75}$$

where

$$c_3 = \rho_{u1} - c_1, \tag{76}$$

$$c_4 = (1 + (1 - \phi_e)c_1)(c_2 - \rho_{u1}) + \rho_{u1} - c_1. \tag{77}$$

Furthermore, we can obtain the second derivative of $G(\phi_2)$ with respect to ϕ_2 as $G(\phi_2)''$, which is give by

$$G(\phi_2)'' = \frac{\partial G(\phi_2)'}{\partial \phi_2} = -\frac{1}{\ln(2)} \frac{c_1(2 - \phi_e)((N-1)\beta_2 \rho_{u2} + \rho_{u2} - \rho_{u1})}{(1 + \phi_2 \rho_{u1})^3} < 0, \tag{78}$$

due to the facts $\phi_e < 1$ and $\rho_{u1} \leq \rho_{u2}$. Following (78), we find that $G(\phi_2)$ is a concave function of ϕ_2 , which completes the proof of Lemma 3.

APPENDIX C

PROOF OF LEMMA 4

Following (57), we derive the first derivative of $\phi_1 (1 + (1 - \phi_1 - \gamma_1)\rho_e)^K \triangleq Q(\phi_1)$ with respect to ϕ_1 as

$$\begin{aligned} Q(\phi_1)' &\triangleq \frac{\partial(\phi_1 (1 + (1 - \phi_1 - \gamma_1)\rho_e)^K)}{\partial\phi_1} \\ &= ((1 + (1 - \phi_1 - \gamma_1)\rho_e)^{K-1} (((1 + (1 - \phi_1 - \gamma_1)\rho_e) - K\phi_1\rho_e)). \end{aligned} \quad (79)$$

Following (79) and noting $1 - \phi_1 - \gamma_1 \geq 0$, we have

$$\phi_1 = \phi_1^\dagger \triangleq \frac{1 + \rho_e - \gamma_1\rho_e}{(K + 1)\rho_e}, \quad (80)$$

in order to guarantee $Q(\phi_1)' = 0$. As per (79), we can find that $Q(\phi_1)' > 0$ for $\phi_1 < \phi_1^\dagger$, which indicates that the function of $Q(\phi_1)$ is a monotonically increasing function of ϕ_1 when $\phi_1 < \phi_1^\dagger$. We also find that $Q(\phi_1)' < 0$ for $\phi_1 > \phi_1^\dagger$, which shows that the function of $Q(\phi_1)$ is a monotonically decreasing function of ϕ_1 when $\phi_1 > \phi_1^\dagger$. As such, we can conclude that $Q(\phi_1)$ is maximized when $Q(\phi_1)' = 0$, i.e., when (80) is guaranteed. This completes the proof of Lemma 4.

REFERENCES

- [1] Y. Saito, A. Benjebbour, Y. Kishiyama, and T. Nakamura, "System-level performance evaluation of downlink non-orthogonal multiple access (NOMA)," in *Proc. IEEE PIMRC*, London, UK, Sep. 2013, pp. 611–615.
- [2] L. Dai, B. Wang, Y. Yuan, S. Han, C.-L. I, and Z. Wang, "Nonorthogonal multiple access for 5G: Solutions, challenges, opportunities, and future research trends," *IEEE Commun. Mag.*, vol. 53, no. 9, pp. 74–81, Sep. 2015.
- [3] Z. Ding, X. Lei, G. K. Karagiannidis, R. Schober, J. Yuan, and V. K. Bhargava, "A survey on non-orthogonal multiple access for 5G networks: Research challenges and future trends," *IEEE J. Select. Areas Commun.*, vol. 35, no. 10, pp. 2181–2195, Oct. 2017.
- [4] Y. Liu, Z. Qin, M. Elkashlan, Z. Ding, A. Nallanathan, and L. Hanzo, "Nonorthogonal multiple access for 5G and beyond," *Proc. IEEE*, vol. 105, no. 12, pp. 2347–2381, Dec. 2017.
- [5] A. Benjebbovu, A. Li, Y. Saito, Y. Kishiyama, A. Harada, and T. Nakamura, "System-level performance of downlink NOMA for future LTE enhancements," in *Proc. IEEE Globecom*, Dec. 2013, pp. 66–70.

- [6] J. Choi, "On the power allocation for MIMO-NOMA systems with layered transmissions," *IEEE Trans. Wireless Commun.*, vol. 15, no. 5, pp. 3226–3237, May 2016.
- [7] Y. Sun, D. W. K. Ng, Z. Ding, and R. Schober, "Optimal joint power and subcarrier allocation for full-duplex multicarrier non-orthogonal multiple access systems," *IEEE Trans. Commun.*, vol. 65, no. 3, pp. 1077–1091, Mar. 2017.
- [8] X. Sun, S. Yan, N. Yang, Z. Ding, C. Shen, and Z. Zhong, "Short-packet downlink transmission with non-orthogonal multiple access," *IEEE Trans. Wireless Commun.*, Early Access, Apr. 2018.
- [9] X. Sun, N. Yang, S. Yan, Z. Ding, D. W. K. Ng, C. Shen, and Z. Zhong, "Joint beamforming and power allocation in downlink NOMA multiuser MIMO networks," *IEEE Trans. Wireless Commun.*, Early Access, Jun. 2018.
- [10] S. Yan, N. Yang, G. Geraci, R. Malaney, and J. Yuan, "Optimization of code rates in SISOME wiretap channels," *IEEE Trans. Wireless Commun.*, vol. 14, no. 11, pp. 6377–6388, Nov. 2015.
- [11] Y. Zou, J. Zhu, X. Wang, and L. Hanzo, "A survey on wireless security: Technical challenges, recent advances, and future trends," *Proc. IEEE*, vol. 104, no. 9, pp. 1727–1765, Sep. 2016.
- [12] T.-X. Zheng, H.-M. Wang, J. Yuan, D. Towsley, and M. H. Lee, "Multiantenna transmission with artificial noise against randomly distributed eavesdroppers," *IEEE Trans. Commun.*, vol. 63, no. 11, pp. 4347–4362, Nov. 2015.
- [13] Y. W. P. Hong, P. C. Lan, and C. C. J. Kuo, "Enhancing physical-layer secrecy in multi-antenna wireless systems: An overview of signal processing approaches," *IEEE Signal Process. Mag.*, vol. 30, no. 5, pp. 29–40, Sep. 2013.
- [14] Y. Feng, Z. Yang, W.-P. Zhu, Q. Li, and B. Lv, "Robust cooperative secure beamforming for simultaneous wireless information and power transfer in amplify-and-forward relay networks," *IEEE Trans. Veh. Technol.*, vol. 66, no. 3, pp. 2354–2366, Mar. 2017.
- [15] Y. Feng, S. Yan, Z. Yang, S. Yan, N. Yang, and W.-P. Zhu, "TAS-Based incremental hybrid decode-amplify-forward relaying for physical layer security enhancement," *IEEE Trans. Commun.*, vol. 65, no. 9 pp. 3876–3891, Sep. 2017.
- [16] N. Yang, L. Wang, G. Geraci, M. ElKashlan, J. Yuan, and M. Di Renzo, "Safeguarding 5G wireless communication networks using physical layer security," *IEEE Commun. Mag.*, vol. 53, no. 4, pp. 20–27, Apr. 2015.
- [17] N. Yang, S. Yan, J. Yuan, R. Malaney, R. Subramanian, and I. Land, "Artificial noise: Transmission optimization in multi-input single-output wiretap channels," *IEEE Trans. Commun.*, vol. 63, no. 5, pp. 1771–1783, May 2015.
- [18] Z. Ding, Z. Zhao, M. Peng, and H. V. Poor, "On the spectral efficiency and security enhancements of NOMA assisted multicast-unicast streaming," *IEEE Trans. Commun.*, vol. 65, no. 7, pp. 13151–3163, Jul. 2017.
- [19] Z. Qin, Y. Liu, Z. Ding, Y. Gao, and M. ElKashlan, "Physical layer security for 5G non-orthogonal multiple access in large-scale networks," in *IEEE ICC*, May 2016, pp. 1–6.
- [20] Y. Zhang, H.-M. Wang, Q. Yang, and Z. Ding, "Secrecy sum rate maximization in nonorthogonal multiple access," *IEEE Commun. Lett.*, vol. 20, no. 5, pp. 930–933, May 2016.
- [21] F. Zhou, Z. Chu, H. Sun, R. Q. Hu, and L. Hanzo, "Artificial noise aided secure cognitive beamforming for cooperative MISO-NOMA using SWIPT," *IEEE J. Sel. Areas Commun.*, Early Access, Apr. 2018.
- [22] M. Jiang, Y. Li, Q. Zhang, Q. Li, and J. Qin, "Secure beamforming in downlink MIMO non-orthogonal multiple access networks," *IEEE Signal Process. Lett.*, vol. 24, no. 12, pp. 1852–1855, Aug. 2017.
- [23] M. Tian, Q. Zhang, S. Zhao, Q. Li, and J. Qin, "Secrecy sum rate optimization for downlink MIMO nonorthogonal multiple access systems," *IEEE Signal Process. Lett.*, vol. 24, no. 8, pp. 1113–1117, Aug. 2017.

- [24] B. He, A. Liu, N. Yang, and V. K. N. Lau, "On the design of secure non-orthogonal multiple access systems," *IEEE J. Sel. Areas Commun.*, vol. 35, no. 10, pp. 2196–2206, Oct. 2018.
- [25] Y. Liu, Z. Qin, M. ElKashlan, Y. Gao, and L. Hanzo, "Enhancing the physical layer security of non-orthogonal multiple access in large-scale networks," *IEEE Trans. Wireless Commun.*, vol. 16, no. 3, pp. 1656–1671, Dec. 2017.
- [26] L. Lv, Z. Ding, Q. Ni, and J. Chen, "Secure MISO-NOMA transmission with artificial noise," *IEEE Trans. Veh. Technol.*, Early Access, Mar. 2018.
- [27] Y. Zhang, H.-M. Wang, T.-X. Zheng, and Q. Yang, "Energy-efficient transmission design in non-orthogonal multiple access," *IEEE Trans. Veh. Technol.*, vol. 66, no. 3, pp. 2852–2857, Mar. 2017.
- [28] Z. Chen, Z. Ding, P. Xu, and X. Dai, "Optimal precoding for a QoS optimization problem in two-user MISO-NOMA downlink," *IEEE Commun. Lett.*, vol. 20, no. 6, pp. 1263–1266, Jun. 2016.
- [29] S. Yan, X. Zhou, N. Yang, B. He, and T. D. Abhayapala, "Artificial-noise-aided secure transmission in wiretap channels with transmitter-side correlation," *IEEE Trans. Wireless Commun.*, vol. 15, no. 12, pp. 8286–8297, Dec. 2016.
- [30] S. Yan, N. Yang, R. Malaney, and J. Yuan, "Transmit antenna selection with alamouti coding and power allocation in MIMO wiretap channels," *IEEE Trans. Wireless Commun.*, vol. 13, no. 3, pp. 1656–1667, Mar. 2014.
- [31] Z. Ding, Z. Yang, P. Fan, and H. Poor, "On the performance of nonorthogonalmultiple access in 5G systems with randomly deployed users," *IEEE Signal Process. Lett.*, vol. 21, no. 12, pp. 1501–1505, Dec. 2014.
- [32] S. Goel and R. Negi, "Guaranteeing secrecy using artificial noise," *IEEE Trans. Wireless Commun.*, vol. 7, no. 6, pp. 2180–2189, Jun. 2008.
- [33] N. Li, X. Tao, H. Wu, Q. Cui, and J. Xu, "Large-system analysis of artificial-noise-assisted communication in the multiuser downlink: Ergodic secrecy sum rate and optimal power allocation," *IEEE Trans. Veh. Technol.*, vol. 65, no. 9, pp. 7036–7050, Sep. 2016.
- [34] S.-H. Tsai and H. V. Poor, "Power allocation for artificial-noise secure MIMO precoding systems," *IEEE Trans. Signal Process.*, vol. 62, no. 13, pp. 3479–3493, Jul. 2014.
- [35] N. Li, X. Tao, and J. Xu, "Artificial noise assisted communication in the multiuser downlink: Optimal power allocation," *IEEE Commun. Lett.*, vol. 19, no. 2, pp. 295–298, Feb. 2015.
- [36] Y. Sun, D. W. K. Ng, J. Zhu, and R. Schober, "Robust and secure resource allocation for full-duplex MISO multi-carrier NOMA systems," *IEEE Trans. Wireless Commun.*, Early Access, Jun. 2018.